

Preparation and Characterization of Textile-Grade Long Cellulose Fibers and Their Yarns from Windmill Palm

Changjie Chen,^{a,b} Pengfei Xu,^a Zhong Wang,^c Jingjing Shi,^c Guohe Wang,^c and Xinhou Wang^{b,d,*}

Windmill palm fiber (WPF) is an abundant source of cellulose fiber that can be used in textile manufacturing. In this study, acid-alkali palm fiber and acid-alkali-enzyme palm fiber were prepared to create blended yarns. The morphology, chemical composition, physical structural parameters, and tensile properties of the WPF samples and yarns were studied. The results indicated that both the acid-alkali and acid-alkali-enzyme treatments can be used as degumming methods to prepare windmill palm textile-grade long fibers with spinning ability. After chemical treatment, the cellulose content of WPF increased to more than 60%, up from 34%. However, the line densities of the acid-alkali and acid-alkali-enzyme textile-grade long fibers decreased to 5.29 ± 1.00 tex and 4.52 ± 0.82 tex, respectively. For the enzyme-treated fiber, a stratification phenomenon of the fiber cell walls and a decrease in the modulus were observed. The palm/cotton yarn had a high tensile strength and strip uniformity.

DOI: 10.15376/biores.17.4.5667-5678

Keywords: Windmill palm textile-grade fiber; Palm/cotton yarn; Degumming; Enzyme treatment; Cell wall

Contact information: a: College of Textiles, Donghua University, Shanghai 201620, China; b: Key Laboratory of Textile Science & Technology, College of Textiles, Donghua University, Ministry of Education, China; c: College of Textile and Clothing Engineering, Soochow University, Suzhou, 215006, China; d: College of Mechanical Engineering, Donghua University;

* Corresponding author: xhwang@dhu.edu.cn

INTRODUCTION

The palm tree is an important agricultural crop due to the export of highly demanded palm oil. However, palm trees produce a substantial amount of lignocellulosic agricultural waste. Every year, approximately 40 million tons of byproducts from oil palm species are processed in Malaysia in the form of empty fruit bunches, fronds, and shells (Goh *et al.* 2010, Sabiha-Hanim *et al.* 2011). Notably, Saudi Arabia generates more than 30,000 tons of date-palm leaf and trunk waste (Alotaibi *et al.* 2019). In 2022, more than 28000 tons of windmill palm materials were produced in Sinan city, Yunnan province (Ma *et al.* 2020). Windmill palm trees have attracted increasing interest in recent years owing to their ability to grow in karst microhabitats, including rocky troughs, rocky soil surfaces, and soil surface microhabitats (Liu *et al.* 2020). Therefore, windmill palm tree farming has increased rapidly in southeast China. The planting area of windmill palm trees in the Guizhou province is estimated to exceed 200,000 hectares, providing windmill palm residues of more than 3 million tons.

Global fiber production has accelerated, and the textile industry's output surpassed 100 million tons for the first time in 2016 (Aizenshtein 2018). Synthetic textiles currently encompass 62% of the market (Royer *et al.* 2021). China produces more than half of the

world's textiles. Furthermore, fiber production exceeds 60 million tons, including 58 million tons of synthetic fiber (Li *et al.* 2020). Less than 10% consumption fiber for fabric marketing is natural fiber, while more than 90% consumption fiber for textile is synthetic fibers. The synthetic textiles that are derived from nonrenewable petroleum resources show very limited degradation in the environment. Synthetic textile fibers are most likely to accumulate rapidly over time, which can negatively affect exposed marine organisms and their contribution to ecosystem services (Royer *et al.* 2021). The pollution of micro-plastics from the cracking and erosion of synthetic textiles seriously threatens marine life and human health. Therefore, it is urgent to replace synthetic fibers with naturally degradable fibers.

The lack of natural fiber raw materials is an important factor that affects the production of natural textiles. Therefore, researchers are constantly exploring new natural fiber materials that are ideal for textile production. In addition to the well-known mature plants such as sisal (Liu *et al.* 2018), hemp (Padovani *et al.* 2019), bamboo (Chen *et al.* 2020), and banana fiber (Bhuvaneshwari *et al.* 2017), there are a few uncommon plants that can be used as the sources of cellulose fiber. Natural cellulose castor oil bast fibers with a diameter of 14 to 31 μm and a length of 1,300 to 10,000 μm were extracted using aqueous alkaline media (Gedik 2021). Shaker *et al.* (2020) prepared *Vernonia elaeagnifolia* fiber with a linear density of approximately 25 tex as a possible textile fiber. Another study found that *Typha elephantina* Roxb. can produce fibers with a linear density of approximately 5 tex for textile applications (Haq *et al.* 2021). Only the midrib of the date palm has been studied as a long textile fiber in the Palmae family, despite the fact that there are more than 2,800 species (Sudiono and Susanto 2021) of palm fiber. Although the diameter of the date midrib fiber is approximately 300 μm (Elseify *et al.* 2020), it is considerably higher than that of the natural fibers such as cotton (10 μm), wool (15 to 40 μm), and silk (10 μm) that are used in textile processing. A thorough review of the literature indicates that no research on the long textile-grade WPF has been reported thus far, let alone to produce palm fiber/cotton yarn.

In this study, long textile-grade WPFs and their blended yarns were prepared. The extraction, processing, and characterization of these materials will promote the transformation of the abundant waste WPFs into a useful resource for textile production.

EXPERIMENTAL

Materials

Windmill palm meshes and raw palm fibers

Palm trunk is covered with palm leaf sheath, also called windmill palm mesh, which is mainly comprised of palm fibers and parenchyma cells. The windmill palm meshes as the raw materials for this study were purchased in the Anhui province in China.

Raw WPFs can be extracted from the meshes. First, the palm meshes were opened and graded. Then, the WPFs with different diameters were separated. In this study, thick fibers (greater than 500 μm in diameter) were not included. Moreover, the material in the middle layer of the mesh was selected as the raw material for subsequent refinement and softening treatments.

Windmill palm textile-grade long cellulose fibers (WPCFs)

The WPFs were extracted from the meshes, cut into 5 cm pieces, and used as the

raw material for the subsequent treatment. Acid treatment was used as a pretreatment to remove lignin and make the following degumming process easier. Figure 1 presents the fiber treatment method. First, the palm fibers were treated with 1.5 wt.% of sulfuric acid (H_2SO_4) for 1 h at 80 °C. Then, the palm fibers were treated with 1.5 wt.% sodium hydroxide (NaOH) and 1.6 wt.% hydrogen peroxide (H_2O_2) with a bath ratio of 1:160 at 80 °C for 1 h. After the alkali treatment, the WPFs were washed and filtered. The oven-dried fibers were then separated into two parts. One part was used as the acid-alkali WPCFs to prepare the yarns, and the other part was treated with pectinase. The latter part was treated with 0.2 wt.% pectinase at a pH of 5 at 60 °C for 1 h.

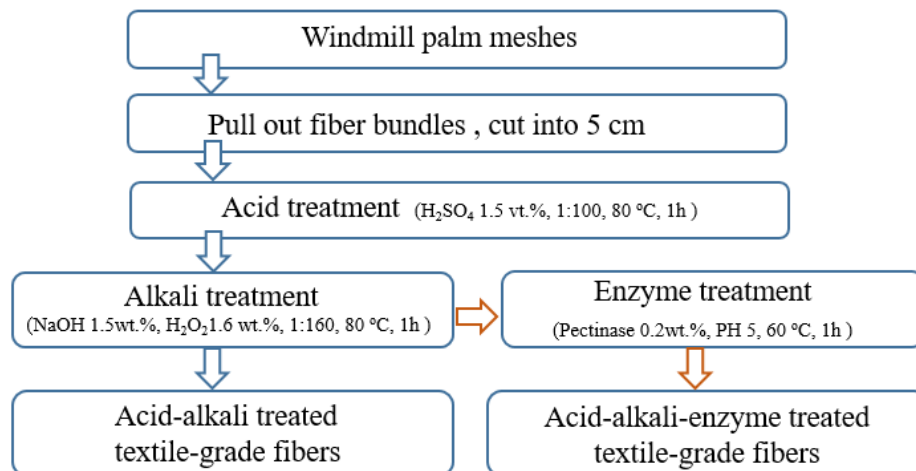


Fig. 1. Process flow for the preparation of the WPCFs from windmill palm meshes

Windmill palm/cotton yarns

Figure 2 shows that the WPCFs extracted *via* the acid-alkali and acid-alkali-enzyme treatments were blended with cotton and spun into yarns through ring spinning. The process followed the steps of blending, carding, drawing, roving, and spinning.

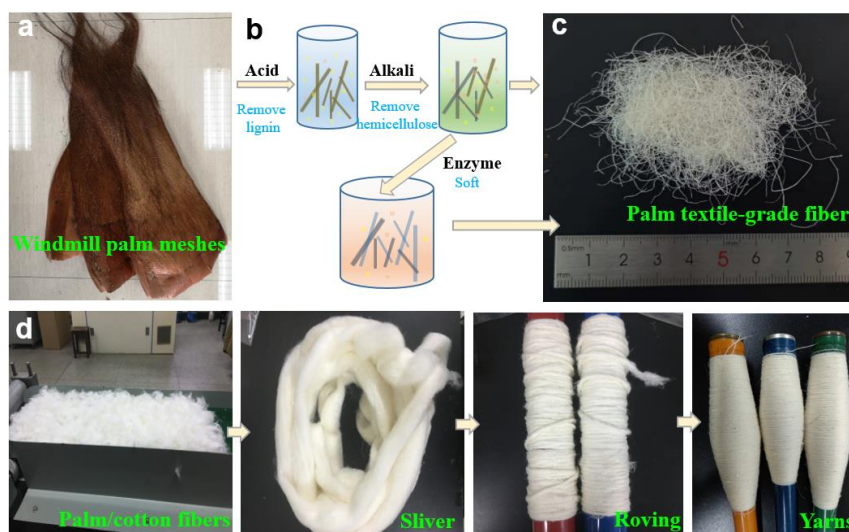


Fig. 2. The process section of the windmill palm/cotton yarns including the a) raw materials, b) chemical treatment of the palm fibers, c) WPCFs, and d) spinning process of blending, sliver, roving, and yarn

Methods

Analysis of the main chemical compositions

The chlorite method was used to determine the holocellulose content of the WPF samples. A total of 5 g of oven-dried palm fibers were weighed and 100 mL of a solution containing a mixture of 2 wt.% of sodium chlorite (NaClO_2), and 0.8 % of acetic acid was added. The vessel containing the resulting liquid mixture was immersed in a water bath at 70 °C for 4 h. This bleaching process was repeated three times to ensure that the lignin was completely removed. The washed and filtered holocellulose was divided into two parts.

One part of the holocellulose was oven-dried at 60 °C for 6 h and weighed to determine the holocellulose content. The holocellulose content was calculated by dividing the mass of the dried holocellulose fiber by the seed amount of fiber before treatment. The other part of the holocellulose fiber was treated with a 17.5 % NaOH solution for 45 min to remove the hemicellulose. The process was then ceased by the addition of distilled water. The α -cellulose content was calculated by subtracting the hemicellulose content from the holocellulose content. The TAPPI T222 om-11 (2011) standard was used to determine the lignin content (Chen, Sun *et al.* 2017).

Fineness of the WPFs

The fineness of the WPCFs and palm/cotton yarns was calculated in terms of their linear density (tex) by measuring the mass (g) of the materials at a certain length (1,000 m) (Shaker, Khan *et al.* 2020). For calculating the linear density of the WPCFs, the weight of more than 300 fibers with a 10 mm length was determined.

Characterization of the WPF samples

The morphologies of the WPF bundles, WPCFs with different treatments, and windmill palm/cotton yarns at microscale were studied using scanning electron microscopy (SEM) images using a Hitachi S-4800 (Tokyo, Japan). The samples were oven-dried and then mounted on an aluminum stub. To improve the conductivity, the surface of these WPF samples was gold-sputtered (E-1045; Hitachi, Tokyo, Japan). The specimens were observed and recorded at 50 \times to 500 \times magnification with a 15-kv accelerating voltage. The diameters of the WPCFs were analyzed using Image J software (open source).

Atomic force microscopy (AFM)

The AFM analysis was performed using dimension edge with high-performance AFM tool (multimode8&bioscope, Veeco, USA) and the Bruker nanoscope analysis software (nanoscope analysis 1.5, Billerica, MA, USA). An ultramicrotome was used to cut ultrathin slices of the resin-embedded WPFs. The cross sections of these sliced samples of the windmill palm were scanned in the machine's tapping mode at a scan rate of 1 Hz.

Tensile test

The tensile strength and strain at break of the WPFs and palm/cotton yarns were determined using the ASTM D3822 (2001) standard. The WPF samples were mounted between two paper frames and bonded together using epoxy adhesive with a gauge length of 30 mm. The palm/cotton yarn had a gauge length of 20 cm. The tensile test was conducted with an Instron 5967 universal testing machine (Norwood, MA, USA) at a 0.5 mm/min strain rate and a zero starting load (Chen *et al.* 2017). More than 50 specimens were tested per sample. The corresponding numbers of all the samples after the tensile fracture were added. A super depth microscope was used to estimate the fiber cross-

sectional area by tracing the edge of the fiber cross-section. The strength of each sample was calculated by dividing its tensile force by its cross-sectional area. The yarn had a fineness of 24 metric count.

Yarn quality

The windmill palm and cotton blended yarns were placed in a room with continuous temperature (20 °C) and humidity (65%) for 24 h. The Uster evenness tester (ME100, Shanghai, China) was used to assess the quality parameters such as unevenness, coefficient variation, and hairiness at a testing speed of 50 m/min and a testing time of 2 min.

RESULTS AND DISCUSSION

The Structure of the Windmill Palm Mesh

Figure 3 illustrates the three-dimensional (3D) structure of the windmill palm mesh. Generally, the appearance and shape of the palm fibers in different directions showed obvious differences. The fibers with a medium diameter were arranged at an angle with the second layer fibers with a thick diameter on the mesh's surface. The thick fibers, which frequently did not interweave between them (Fig. 3d), were generally connected by parenchymal cells. The thick fibers and medium fibers were bonded together by thin fibers to form a multilayer structure, resulting in a 3D configuration of mesh in space. The third type of fine fiber had an arrangement direction that was irregular, interwoven among numerous layers, and the separated fibers were connected to form a complex network structure.

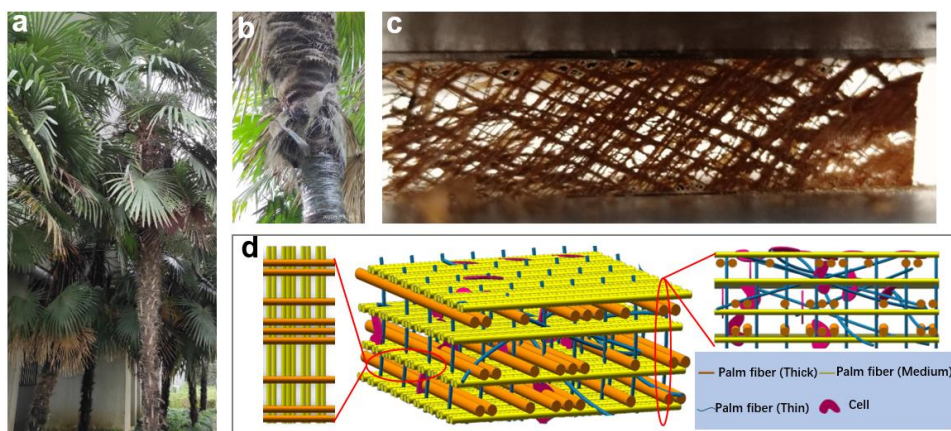


Fig. 3. Images of the a) windmill palm tree, b) mesh attached to the palm trunk, c) sheath mesh, and d) 3D arrangement of the WPF in the sheath mesh

Morphology of the WPFs and yarns

The micro-diameter structure of the raw and treated WPFs, palm fibers, and cotton yarns can be seen in Fig. 4. The raw windmill palm materials had a diameter of more than 400 μm (Fig. 4a), which was 40 times greater than that of cotton fiber and 20 times greater than that of wool fiber. Micro-dimension (5 μm to 10 μm) polygonal silica was placed in a regular arrangement on the surfaces. Simultaneously, crater-shaped annular pits were randomly distributed on the fiber cell wall as a result of physical friction during the drafting process of the fiber bundles.

The diameters of the WPCFs were less than those of the raw materials. Impurities such as silica on the surface, as well as the majority of the fiber's lignin and hemicellulose, were removed after the acid-alkali treatment. Some of the fibers with larger diameter threads were divided into several smaller fibers. The chemical degumming and the physical splitting reduced the fineness of the material, with a diameter of approximately 100 μm (Fig. 4b). A slightly smoother surface was observed in the acid-alkali treated WPCFs, while the enzyme treatment caused some damage to the single fiber cell wall in the WPCF. These differences in WPCFs could be attributed to pectinase's subsequent degradation of the fiber cell wall. Following the acid-alkali-enzyme treatment, the material was further refined to a diameter of approximately 80 μm (Fig. 4c).

Figure 4d illustrates the morphology of the palm/cotton yarns. It was the twisting that tightly mixed and entangled the blended palm fibers and cotton fibers into a continuous material with a slender appearance. The addition of palm fibers somewhat affected the uniformity of yarn fineness. The presence of WPCFs on the surface of the yarns in Figs. 4e and 4f indicated the spinning ability.

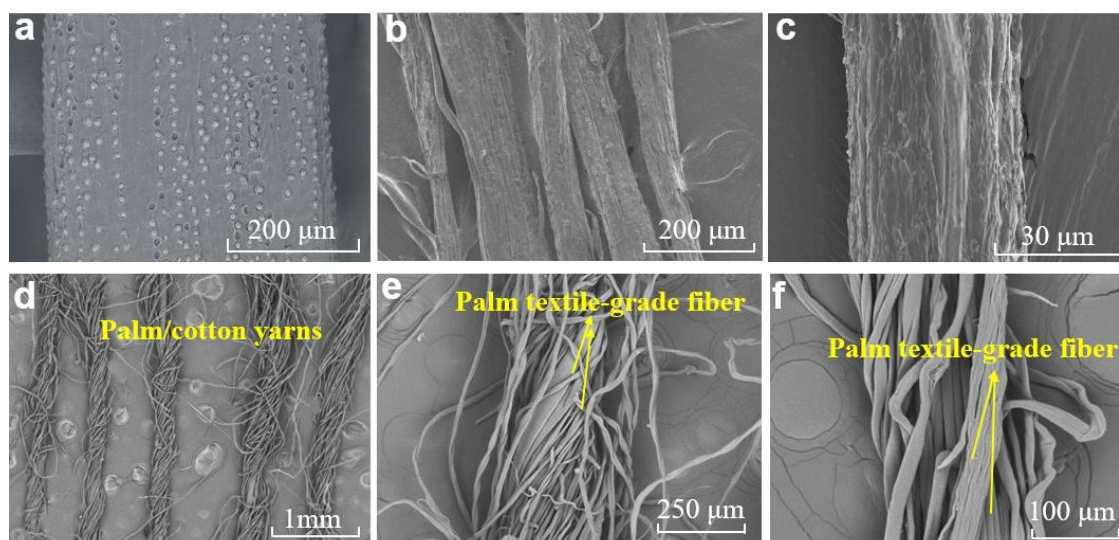


Fig. 4. The SEM images of the longitudinal section for the a) untreated WPFs, b) acid-alkali treated WPFs, c) acid-alkali-enzyme treated WPFs, d) palm/cotton yarns, e) enlarged view of the palm textile-grade fiber, and f) further enlarged view of the palm textile-grade fiber

Analyses of the AFM images of the WPF materials

Figure 5 illustrates the WPF bundle as the raw material and the WPCFs with different treatments. These samples were multicellular fibers. Numerous elementary fibers with an average diameter of approximately 10 μm were combined to generate larger diameter fiber bundles. The cell wall of the elementary palm fiber was approximately 3 μm thick. The cell walls of palm trees still have a hierarchical structure with more than two layers (Zhai *et al.* 2013; Li *et al.* 2020). The S₁ and S₂ layers were clearly visible in the AFM images. The thickness of these samples was almost unchanged. The thickness of the S₁ and S₂ layers were approximately 0.8 μm and 1.5 μm , respectively. An important layer for fibers is the S₂, which primarily determines the mechanical properties of the fiber (Mukhtar *et al.* 2016).

Figure 5 illustrates the microstructure of the cross section of three elementary fibers. The raw WPF has a dense cell wall without an interval between the different layers,

while the chemical treatment of the WPCFs increased the space between the S₁ and S₂ layers. This indicated that the chemical treatment had an influence on the microstructure of the cell wall. The interlayer gap is a kind of defect that may be one of the reasons for the decrease in the breaking strength of materials.

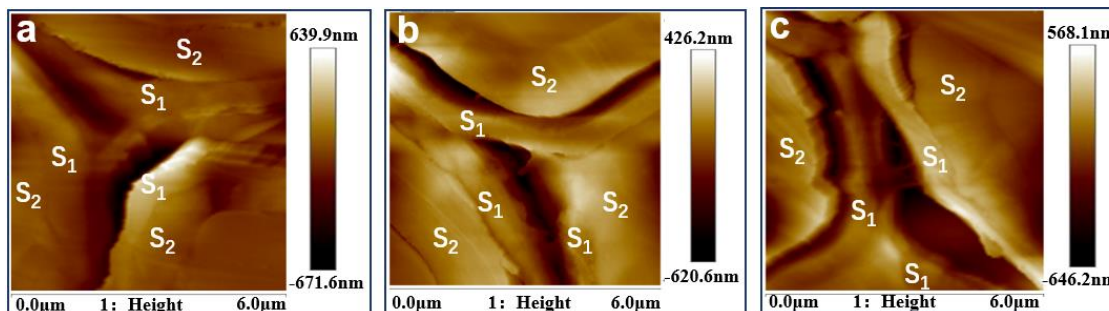


Fig. 5. The cross-section microstructure of the a) untreated, b) acid-alkali treated, and c) acid-alkali-enzyme treated WPF samples under AFM.

The physical and chemical structure of different windmill palm materials

Table 1 provides a comparative analysis of the tensile properties of the raw WPF and the WPCFs. The chemical treatment decreased the tensile properties by reducing the strength and elongation. One of the most fundamental reasons for the reduced tensile property of yarn is the lower tensile strength of the pectinase-treated WPCFs. The enzyme treatment improves the softness of the fiber by reducing the modulus of the WPCF, which may contribute to the lessened hairiness. Without enzyme treatment, WPCF had improved tensile properties due to reduced degradation of the fiber structure both on the cell wall surface and in the cross section of the S₁ and S₂ layers.

The chemical composition of the most important tree species that produces lignocellulose fibers was studied. The chemical treatment increased the α -cellulose content of the palm fiber from 34.2% to well above 60%. In contrast, the contents of lignin and hemicellulose were reduced to different degrees. The fact that the acid-alkali-enzyme-treated palm fiber had the lowest hemicellulose and lignin content indicates that the enzyme treatment further degrades the non-cellulose substances. As a result, the linear density of the fiber after enzyme treatment gradually decreased to 4.52 ± 0.82 tex, roughly one-third of that of the untreated fiber.

Table 1. The Physical Properties of the WPFs with Different Treatments

| Sample | Diameter (μm) | Linear Density (tex) | α -cellulose (%) | Hemi-cellulose (%) | Lignin (%) | Modulus (cN/dtex) | Elongation (%) |
|--------------------|----------------------------|----------------------|-------------------------|--------------------|------------|---------------------|---------------------|
| Untreated | 360.21 ± 41.94 | 11.94 ± 2.67 | 34.2 | 29.1 | 20.8 | 36.51 ± 3.78 | 30.15 ± 4.23 |
| Acid-alkali | 102.37 ± 5.29 | 5.29 ± 1.00 | 60.2 | 25.1 | 12.3 | 30.27 ± 2.01 | 18.45 ± 3.42 |
| Acid-alkali-enzyme | 86.30 ± 4.52 | 4.52 ± 0.82 | 63.5 | 18.1 | 10.3 | 21.73 ± 1.98 | 16.70 ± 3.64 |

The quantity of the palm/cotton yarns

Figure 6 illustrates the evenness of windmill palm and cotton yarns. The acid-alkali palm/cotton yarn's unevenness (U) and variable coefficient (CV) of acid-alkali palm/cotton yarn were 21.4% and 28.2%, respectively. The quality of the WPCF yarn after the enzyme treatment showed noticeable improvement, and the U, CV, and deviation rate all decreased notably. The increased softness of the enzyme-treated WPCFs made them easy to transfer inside and outside the yarn triangle, which allowed the palm fiber to penetrate the yarn and reduced the U and CV of the yarn to 17.2% and 23.0%, respectively.

Hairiness is an important criterion for determining the yarn quality. The length and number of hairs will affect the efficiency and quality of further processing, in addition to the appearance and style of the fabric. The cumulative total length of the fibers that extend out of the yarn within a length range of 1 cm in millimeters is known as the H-value. The acid-alkali palm/cotton yarn and acid-alkali-enzyme palm/cotton yarn had similar H-values of 7.60 and 7.65, respectively. The significant difference was analyzed according to the T test independent sample. The Sig. value was 0.64, which means that the results for dryness, uniformity, and hairiness of the windmill palm yarn prepared from different treated palm fiber showed no significant difference. Dong *et al.* (2016) created cotton stalk bark/cotton yarn by combining cotton stalk bark and cotton fiber at a 30:70 ratio. They achieved a CV of 28.2 and an H-value of 22.5, which were much higher than the results in this study. This shows that palm blended yarn has better spin ability than cotton stalk leather fiber.

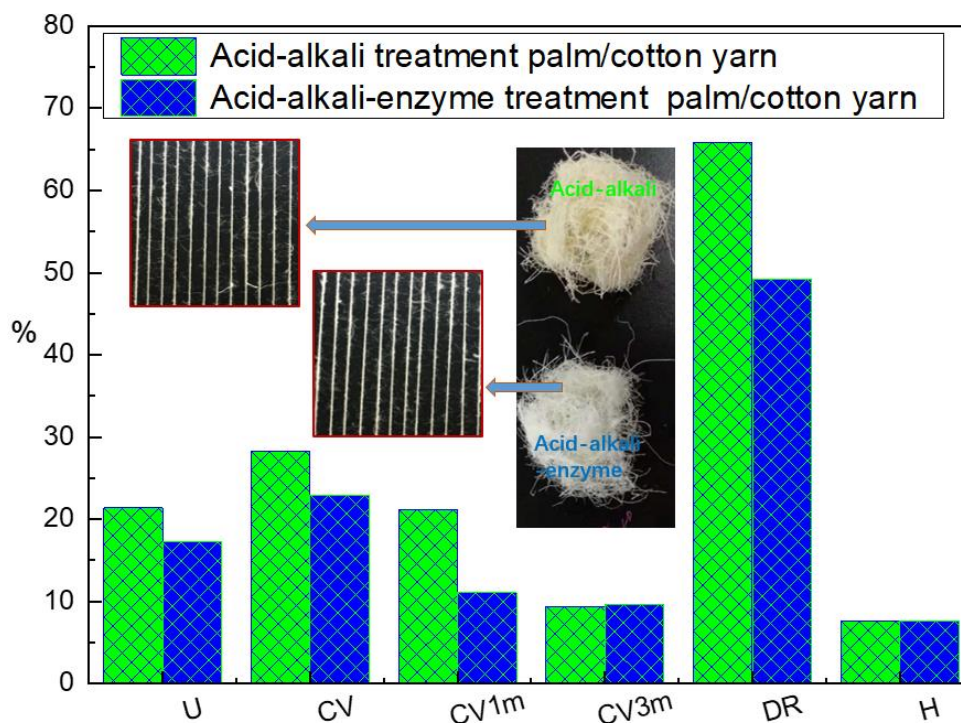


Fig. 6. The dryness, uniformity, and hairiness of the windmill palm yarn

Figure 7 illustrates the defects of the ring spun yarns of acid-alkali palm textile-grade long cellulose palm/cotton 20/80 and acid-alkali-enzyme palm/cotton 20/80 specimens. The higher rigidity of the WPCF without enzyme treatment made the twisting process more difficult to perform. Due to the high drafting ratio, unanticipated thin spots were easily formed in the spinning process elongation. The number of thin spots was

obviously reduced after the enzyme treatment. While the thick spots (35%) of the enzyme-treated yarn had increased slightly, this could be responsible for the worse length uniformity during the further water bath treatment. The increased content of floating fibers decreased the parallel straightness of fibers in the strands. As a result, the irregular hook fibers were tangled in thick places. The defects between the acid-alkali-enzyme palm/cotton yarn and acid-alkali palm/cotton yarn made a big difference, as was apparent from a Sig. value is 0.01. Enzymatic treatment improved the yarn quality.

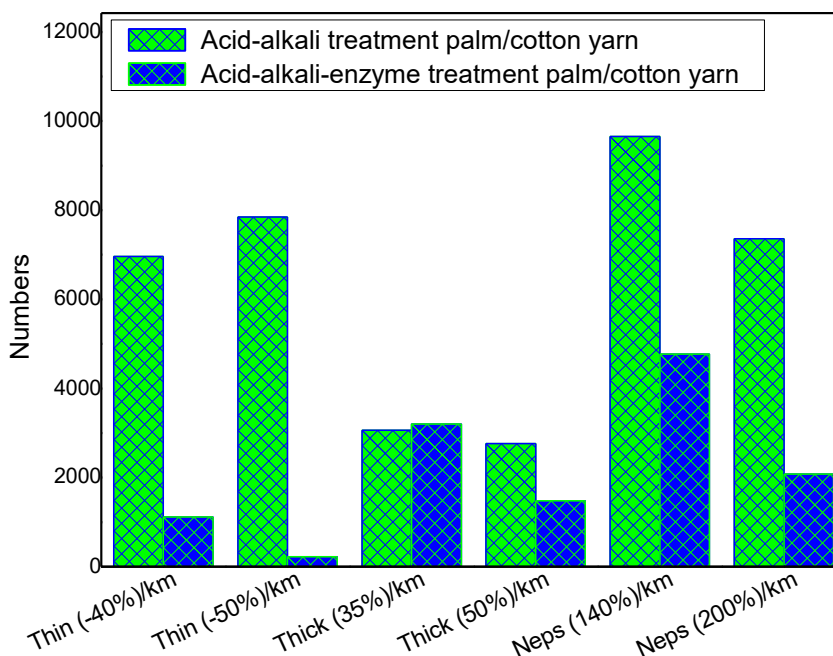


Fig. 7. The defects of the windmill palm yarn

New cellulose fiber materials include banana fiber, pineapple leaf fiber, cotton stalk bark fiber, and palm fiber. Many researchers have combined these fibers with cotton to create yarns. Figure 8 illustrates that the windmill palm/cotton yarns had strong mechanical properties. The tensile strength of the acid-alkali palm/cotton 30/70 yarn had a tensile strength of more than 18 cN/tex, which was significantly higher than that of the banana/cotton 20/80 yarn (5.5 cN/tex) (Ortega *et al.* 2016), the antibacterial polyester fiber/lyocell/long staple cotton/pineapple fiber 30/25/25/20 yarn (14.77 cN/tex) (Li *et al.* 2016) and the cotton stalk bark/cotton yarn 30/70 (14.1 cN/tex) (Dong *et al.* 2016). As illustrated in Fig. 8, the remarkable tensile strength decreased from 18.36 cN/tex to 10.25 cN/tex of palm/cotton yarn after the enzyme treatment. This was consistent with the decrease in process fiber strength following enzyme treatment. The elongation at break was approximately 8%, which was nearly the same for the acid-alkali palm/cotton yarn and the acid-alkali-enzyme palm/cotton yarn. From the statistical point of view, there was no significant difference in mechanical properties between the two yarns, since the Sig. value was 0.19, which is higher than 0.05. One of the important properties of weaving's use is its mechanical properties. The palm/cotton yarn was suitable for the textile created through weaving and processing fabric.

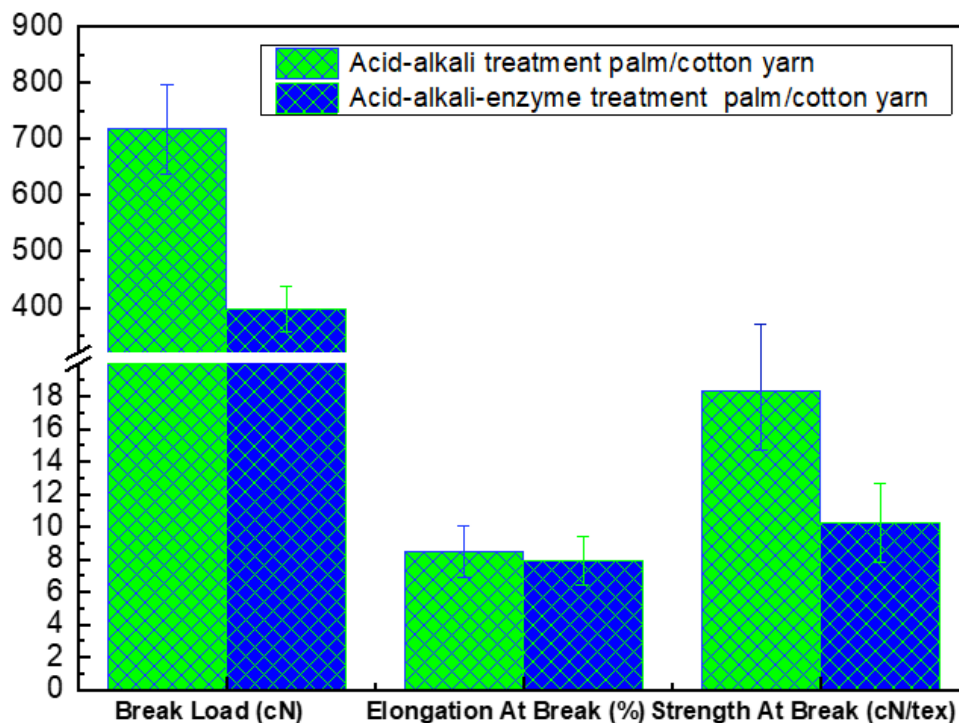


Fig. 8. The mechanical properties of the windmill palm yarn

CONCLUSIONS

1. As an abundant commercial plant, the windmill palm tree can be a source of palm fiber with a high cellulose content and good mechanical properties.
2. Although the stiffness and wide range in diameter of windmill palm textile-grade long cellulose fibers (WPCFs) have hampered their application in textiles for thousands of years, a chemical treatment can be used to extract WPCFs with spinning ability.
3. After the chemical treatment, the contaminants on the fiber surface were removed. The acid-alkali-enzyme-treated WPCF had a high cellulose content of 63.47%, a fine linear density of 4.52 tex, and a soft mechanical property with a modulus of 21cN/dtex.
4. Spinning was able to successfully produce high-quality palm/cotton 20/80 blended yarns. The enzyme treatment increased the quality of the palm and cotton yarns by decreasing the U, CV, H, and defect levels.

ACKNOWLEDGMENTS

This research was funded by the Fundamental Research Funds for the Central Universities (2232020D-16), Funding for the Young Teachers' Scientific Research (101-20-000101), and the National Natural Science Foundation of China (51776034).

REFERENCES CITED

- Aizenshtein, E. M. (2018). "Global production and consumption of chemical fibres in 2016," *Fibre Chemistry* 50(1), 73-78. DOI: 10.1007/s10692-018-9934-y
- Alotaibi, M. D., Alshammari, B. A., Saba, N., Alothman, O. Y., Sanjay, M. R., Almutairi, Z., and Jawaid, M. (2019). "Characterization of natural fiber obtained from different parts of date palm tree (*Phoenix dactylifera* L.)," *International Journal of Biological Macromolecules* 135, 69-76. DOI: 10.1016/j.ijbiomac.2019.05.102
- ASTM D3822 (2007). "Standard test method for tensile properties of single textile fibers," ASTM International, West Conshohocken, PA.
- Bhuvanewari, H. B., Vinayaka, D. L., Ilangovan, M., and Reddy, N. (2017). "Completely biodegradable banana fiber-wheat gluten composites for dielectric applications," *Journal of Materials Science-Materials in Electronics* 28(17), 12383-12390. DOI: 10.1007/s10854-017-7058-4
- Chen, C., Chen, G., Li, X., Guo, H., and Wang, G. (2017). "The influence of chemical treatment on the mechanical properties of windmill palm fiber," *Cellulose* 24(4), 1611-1620. DOI: 10.1007/s10570-017-1205-1
- Chen, C., Li, Z., Mi, R., Dai, J., Xie, H., Pei, Y., Li, J., Qiao, H., Tang, H., Yang, B., *et al.* (2020). "Rapid processing of whole bamboo with exposed, aligned nanofibrils toward a high-performance structural material," *ACS Nano* 14(5), 5194-5202. DOI: 10.1021/acsnano.9b08747
- Chen, C., Sun, G., Chen, G., Li, X., and Wang, G. (2017). "Microscopic structural features and properties of single fibers from different morphological parts of the windmill palm," *BioResources* 12(2), 3504-3520. DOI: 10.15376/biores.12.2.3504-3520
- Dong, Z., Hou, X., Haigler, I., and Yang, Y. (2016). "Preparation and properties of cotton stalk bark fibers and their cotton blended yarns and fabrics," *Journal of Cleaner Production* 139, 267-276. DOI: 10.1016/j.jclepro.2016.08.035
- Elseify, L. A., Midani, M., Hassanin, A. H., Hamouda, T., and Khiari, R. (2020). "Long textile fibres from the midrib of date palm: Physiochemical, morphological, and mechanical properties," *Industrial Crops and Products* 151, article no. 112466. DOI: 10.1016/j.indcrop.2020.112466
- Gedik, G. (2021). "Extraction of new natural cellulosic fiber from *Trachelospermum jasminoides* (star jasmine) and its characterization for textile and composite uses," *Cellulose* 28(11), 6899-6915. DOI: 10.1007/s10570-021-03952-1
- Goh, C. S., Tan, K. T., Lee, K. T., and Bhatia, S. (2010). "Bio-ethanol from lignocellulose: Status, perspectives and challenges in Malaysia," *Bioresource Technology* 101(13), 4834-4841. DOI: 10.1016/j.biortech.2009.08.080
- Haq, U. N., Huraira, A., and Uddin, M. A. (2021). "Physical characteristics of *Typha elephantina* Roxb. fiber (*Hogla*) for textile application," *Journal of the Textile Institute* DOI: 10.1080/00405000.2021.1981020
- Li, J., Zhang, X., Zhu, J., Yu, Y., and Wang, H. (2020). "Structural, chemical, and multi-scale mechanical characterization of waste windmill palm fiber (*Trachycarpus fortunei*)," *Journal of Wood Science* 66(1). DOI: 10.1186/s10086-020-1851-z
- Li, Y., Li, F., Li, X., and Zhang, Y. (2016). "Spinning process research of pineapple blended fiber knitting yarn," *Journal of Qingdao University (Engineering & Technology Edition)* 3, 119-122.
- Li, C., Zhao, R., and Lu, X. (2020). "2019 review and 2020 outlook for world and China

- synthetic fiber industry,” *Petroleum & Petrochemical Today* 28(4), 14-17.
- Liu, K., Wang, Y., Cheng, P., Liu, Y., Kong, C., Yi, Z., Li, M., Liu, Q., Zhong, Q., Takagi, H., *et al.* (2018). “Nanosized nickel decorated sisal fibers with tailored aggregation structures for catalysis reduction of toxic aromatic compounds,” *Industrial Crops and Products* 119, 226-236. DOI: 10.1016/j.indcrop.2018.04.031
- Liu, Y., Wei, X., Zhou, Z., Shao, C., and Su, S. (2020). “Influence of heterogeneous karst microhabitats on the root foraging ability of Chinese windmill palm (*Trachycarpus fortunei*) seedlings,” *International Journal of Environmental Research and Public Health* 17(2), 434. DOI: 10.3390/ijerph17020434
- Mukhtar, I., Leman, Z., and Ishak, M. R. (2016). “Sugar palm fibre and its composites: A review of recent developments,” *BioResources* 11(4), 10756-10782. DOI: 10.15376/biores.11.4.10756-10782
- Ortega, Z., Morón, M., Monzón, M. D., Badalló, P., and Paz, R. (2016). “Production of banana fiber yarns for technical textile reinforced composites,” *Materials* 9(5), 370-375. DOI: 10.3390/ma9050370
- Padovani, J., Legland, D., Pernes, M., Gallos, A., Thomachot-Schneider, C., Shah, D. U., Bourmaud, A., and Beaugrand, J. (2019). “Beating of hemp bast fibres: An examination of a hydro-mechanical treatment on chemical, structural, and nanomechanical property evolutions,” *Cellulose* 26(9), 5665-5683. DOI: 10.1007/s10570-019-02456-3
- Royer, S. J., Wiggin, K., Kogler, M., and Deheyn, D. D. (2021). “Degradation of synthetic and wood-based cellulose fabrics in the marine environment: Comparative assessment of field, aquarium, and bioreactor experiments,” *Science of the Total Environment* 791, 148060. DOI: 10.1016/j.scitotenv.2021.148060
- Sabiha-Hanim, S., Noor, M. A. M., and Rosma, A. (2011). “Effect of autohydrolysis and enzymatic treatment on oil palm (*Elaeis guineensis* Jacq.) frond fibres for xylose and xylooligosaccharides production,” *Bioresource Technology* 102(2), 1234-1239. DOI: 10.1016/j.biortech.2010.08.017
- Shaker, K., Khan, R. M. W. U., Jabbar, M., Umair, M., Tariq, A., Kashif, M., and Nawab, Y. (2020). “Extraction and characterization of novel fibers from *Vernonia elaeagnifolia* as a potential textile fiber,” *Industrial Crops and Products* 152, 112518. DOI: 10.1016/j.indcrop.2020.112518
- Sudiono, J., and Susanto, G. R. (2021). “Antioxidant content of palm fruit (*Borassus flabellifer* L.) seed coat,” *Biomedical Journal of Scientific & Technical Research* 34(3), 26695-26699. DOI: 10.26717/BJSTR.2021.34.005540
- TAPPI T222 om-11 (2011). “Acid-insoluble lignin in wood and pulp,” TAPPI Press, Atlanta, GA.
- Zhai, S., Horikawa, Y., Imai, T., and Sugiyama, J. (2013). “Cell wall characterization of windmill palm (*Trachycarpus fortunei*) fibers and its functional implications,” *IAWA Journal* 34(1), 20-33. DOI: 10.1163/22941932-00000003

Article submitted: April 22, 2022; Peer review completed: May 22, 2022; Revisions received and accepted: June 6, 2022; Published: August 11, 2022.
DOI: 10.15376/biores.17.4.5667-5678